Statistical investigation of the length-dependent deviations in the electrical characteristics of molecular electronic junctions fabricated using the direct metal transfer method

Hyunhak Jeong[1], Dongku Kim[1], Hyukwoo Kwon[1], Wang-Taek Hwang[1], Yeonsik Jang[1], Misook Min[1], Kookrin Char[1], Dong Xiang[2], Heejun Jeong[3] and Takhee Lee[1]

[1] Department of Physics and Astronomy, Institute of Applied Physics, Seoul National University, Seoul 08826, Korea
[2] Key Laboratory of Optical Information Science and Technology, Institute of Modern Optics, College of Electronic Information and Optical Engineering, Nankai University, Tianjin 300071, People's Republic of China
[3] Department of Applied Physics, Hanyang University, Ansan 15588, Korea

E-mail: xiangdongde@126.com, hjeong@hanyang.ac.kr and tlee@snu.ac.kr

Abstract

We fabricated and analyzed the electrical transport characteristics of vertical type alkanethiolate molecular junctions using the high-yield fabrication method that we previously reported. The electrical characteristics of the molecular electronic junctions were statistically collected and investigated in terms of current density and transport parameters based on the Simmons tunneling model, and we determined representative current–voltage characteristics of the molecular junctions. In particular, we examined the statistical variations in the length-dependent electrical characteristics, especially the Gaussian standard deviation σ of the current density histogram. From the results, we found that the magnitude of the σ value can be dependent on the individual molecular length due to specific microscopic structures in the molecular junctions. The probable origin of the molecular length-dependent deviation of the electrical characteristics is discussed.

Keywords: molecular electronics, self-assembled monolayer, metal–molecule–metal junction, statistical analysis, direct metal transfer

S Online supplementary data available from stacks.iop.org/JPhysCM/28/094003/mmedia

(Some figures may appear in colour only in the online journal)

1. Introduction

As a future alternative for conventional Si-based electronics, molecular electronics that utilize functional molecules as active device components have attracted significant attention from both scientific and application points of view. Since the first conceptual model of a molecular rectifier was proposed, interest in the research field has been growing rapidly, and many research groups have extensively studied electronic charge transport through molecular layers with various device

structures to reveal the intrinsic charge transport mechanism and realize real device applications [1–6]. In particular, alkyl-based molecular junctions have been one of the most widely investigated systems to examine transport characteristics because alkyl molecules with specific end groups are known to form stable and well-ordered molecular monolayer films on various substrates (such as Au surfaces) [7, 8]. Despite their abundant virtues compared with conventional microelectronics, molecular electronic device applications have been hampered by many obstacles, preventing reliable, reproducible, and high-yield electronic transport characteristics of molecular systems. To overcome these obstacles and understand genuine charge transport characteristics of the junctions, analyzing a statistically sufficient number of molecular devices is highly desirable because the statistical investigation can single out the accurate characteristics of molecular systems from the ambiguously collected experimental data by observing the statistical distribution of the data. Actually, many research groups have reported these kinds of statistical results [9–11], meanwhile there have been several efforts to achieve high-yield molecular junctions [8, 12, 13]. In most cases, only statistically 'representative' (i.e. averaged) electrical characteristics were treated as crucial parameters, while the deviations of these characteristics from junction to junction did not attract particular attention. Nevertheless, based on the fact that these deviations stem from variations in the specific microscopic structures of the molecular layers, it is worth investigating to gain insight into the structural states of the molecular layers for robust future electronics applications. Therefore, an investigation of the deviations in the electrical characteristics would be beneficial for these purposes.

Here, we analyzed a statistically significant number of alkanethiolate molecular junctions that were fabricated using a previously reported high-yield molecular junction fabrication method as metal–molecule–metal (M–M–M) structures. Statistical analysis with a simple tunneling model was performed, which enabled us to examine basics of the charge transport characteristics through alkanethiolate molecular layers. Specifically, by investigating some transport parameters derived from the modeling, we could obtain a brief insight into the molecular junction structure and molecule-electrode interface. Additionally, the statistical deviations in the electrical characteristics as functions of the molecular length related to the specific molecular junction structures and interfaces have been observed and analyzed.

2. Experimental details

2.A. Device fabrication procedure

Here, we employed the fabrication procedure that we previously reported to generate molecular transport junctions [10, 14]. However, for better understanding, we briefly present the process again. First, the bottom metal electrodes (50 nm Au; 5 nm Ti) were formed using conventional photolithography and the lift-off technique on Si/SiO$_2$ (1.5 cm × 1.5 cm; 100 nm-thick SiO$_2$) substrates. Then, using plasma-enhanced chemical vapor deposition, we deposited 50 nm-thick SiO$_2$

insulating walls that separate the bottom electrodes from the top electrodes. After that, we created circular via-hole structures with various radii (2, 3, 4 and 5 μm) on the insulating layer (SiO$_2$) through photolithography and reactive ion etching to reveal the bottom Au surface on which the molecules will be deposited. Then, self-assembled monolayers (SAMs) of molecules were produced on the bare surfaces of the Au bottom electrodes by dipping the samples into a dilute ethanolic solution (~5 mM) of alkanethiolate molecules for 1–2 d. Here, we used three different alkanethiolate (HS(CH$_2$)$_{n-1}$CH$_3$) SAMs based on their molecular lengths for the molecular junctions, i.e. octanethiol (HS(CH$_2$)$_7$CH$_3$, denoted as C8), dodecanethiol (HS(CH$_2$)$_{11}$CH$_3$, C12), and hexadecanethiol (HS(CH$_2$)$_{15}$CH$_3$, C16), to compare the electrical characteristics because the alkanethiolate molecular junction is the well-established standard molecular junction system that has been extensively investigated in the research field of molecular electronics [7, 8]. After the deposition of alkanethiolate SAMs on the bottom Au surface, the top metal contacts on the molecular layers were produced by following the direct metal transfer (DMT) method that we reported previously [14, 15]. Briefly, we directly transferred a thin metal sheet (15 nm of Au), which was used as the top electrode of the molecular junctions, onto the SAMs. The detailed procedure for preparing the transfer film will be presented in following section. Using this method, the device yield (~70%) was significantly improved with a pure (i.e. interlayer-less) M–M–M junction structure [14]. Figure 1(a) shows microscopic images of our molecular junctions that were collected using optical and scanning electron microscopes (SEM). Figures 1(b) and (c) present schematic illustrations of the vertical junction structures of our molecular devices.

2.B. Transfer film preparation procedure

A patterned, thin Au sheet was utilized as the top electrode and transferred onto the molecular layers similar our previous study [14, 15]. To prepare the film, we followed the steps below: First, we evaporated the top Au electrodes (15 nm) using shadow mask onto a dummy silicone substrate (Si/SiO$_2$ with 100 nm-thick SiO$_2$) with an electron beam evaporator. After the evaporation, we spin-coated (4000 rpm, 1 min) poly(methyl methacrylate) (PMMA; 950 K A4 purchased from MicroChem) onto the dummy substrate as a supporting layer for the top Au electrodes that is possible to be torn when the electrode is detached from the dummy substrate. Then, we attached plastic tape around the substrate to support the thin transfer film layer. After this process, we immersed the entire substrate with the plastic tape into a potassium hydroxide (KOH) solution (~25%, 60 ml) for approximately an hour to detach the top Au electrodes with the thin PMMA layer from the dummy substrate. Here, the KOH solution etches the SiO$_2$ layer so that the film can be detached from the substrate. Finally, the remaining transfer film composed of the top Au electrode and PMMA layer was gently rinsed with deionized water 3–5 times to remove the remaining KOH solution and gently dried under a N$_2$ stream for several hours. After placing these films onto the SAMs, vertical M–M–M junctions were
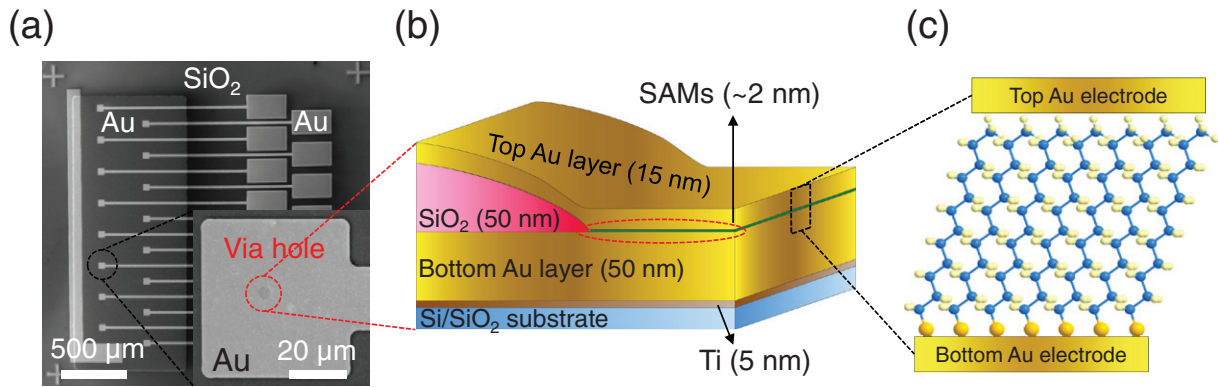
Figure 1. (a) Microscopic images of the fabricated molecular junctions using SEM and optical microscopy. (b, c) Schematic illustration of the molecular junction structure with dodecanethiol (C12) SAMs.

created. Note that, before generating the contact, we applied a few drops of clean isopropyl alcohol (IPA) between the SAMs and the top Au electrode to promote conformal contact, which occurs because the surface tension that is induced as the IPA evaporates results in capillary action between the SAMs and the top Au electrode, allowing the transfer film to make soft and fine contact with the SAMs. Lastly, the supporting PMMA layer was removed by immersing the samples in acetone for ~30 min to expose the top Au electrode surface. For more detailed information about the preparation procedure, please see our previous study [14].

3. Results and discussion

3.A. Fundamental part: Statistical analysis of electrical characteristics and tunneling model

As mentioned in the introduction, examining the electrical characteristics of a statistically significant number of molecular junctions has the virtue of singling out the genuine charge transport properties of molecular junctions from ambiguously collected experimental data. To accomplish this task, we analyzed a large number (approximately 400) of molecular junctions, which are each composed of 128 junctions for C8, C12 and C16 alkanethiolate molecules and fabricated using our DMT method. From these devices, we determined so called 'working' molecular devices which can be recognized as statistically meaningful junctions based on the Gaussian distribution of the electrical characteristics (here current density, J) of the devices. The working devices were defined and selected from the all of the devices based on the criterion that they show statistically similar current densities at certain bias voltage to that of the majority of the devices in the Gaussian distribution, as shown in figure 2(a). For a detailed explanation of the criterion for selecting the working devices, please see our previous reports [10, 14]. In this report, we found that approximately 70% of the devices can be regarded as working devices with M–M–M junction structures, which means 70% of our molecular junctions exhibited molecularly-based electrical characteristics [14].

We can obtain representative *J-V* characteristics by log-averaging the current densities of the working devices as shown in figure 2(b). To plot the graph, we found the
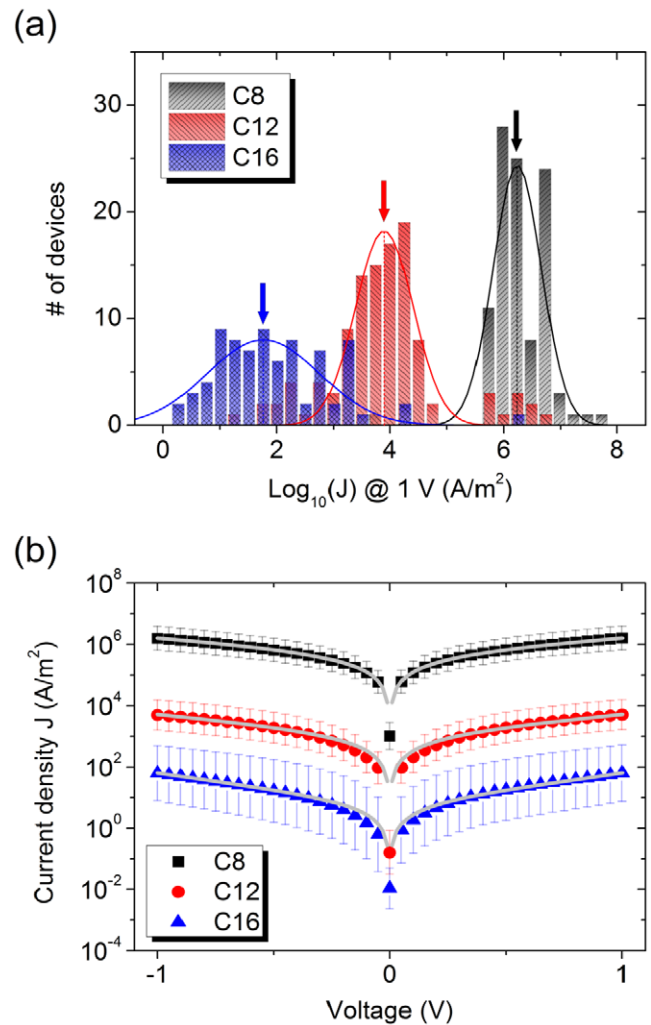
Figure 2. (a) Current density histogram at 1 V bias voltage for all candidate molecular devices. The Gaussian fitting results are shown as solid curves in the plot. (b) Statistically averaged representative *J-V* characteristics for all C8, C12, and C16 working devices. Gray solid curves represent the fitted results using the Simmons tunneling model.

logarithmic current densities of each working device and log-averaged them. Note that the error bars for each data point indicate the Gaussian standard deviations (σ) from the fitting functions of the logarithmic J values of each working device

in figure 2(a). In the following section, we will discuss the length-dependent variations of the σ values in detail. It is widely known from various studies that the charge transport mechanism through alkanethiolate SAMs is non-resonant tunneling transport [16, 17], which can be simply described by the well-known Simmons tunneling model that describes the metal-insulator-metal junction as a rectangular shaped tunneling barrier system [18–20]:

$$J = \left(\frac{e}{4\pi^2\hbar d^2}\right)\left[\left(\Phi_B - \frac{eV}{2}\right)\exp\left\{-\frac{2\sqrt{2m}}{\hbar}\alpha\left(\Phi_B - \frac{eV}{2}\right)^{1/2}d\right\}\right.$$
$$\left.-\left(\Phi_B + \frac{eV}{2}\right)\exp\left\{-\frac{2\sqrt{2m}}{\hbar}\alpha\left(\Phi_B + \frac{eV}{2}\right)^{1/2}d\right\}\right]$$

$$(1)$$

where d is the width of the barrier, m is the electron mass, Φ_B is the barrier height, V is the applied bias voltage, and α is an adjustable unitless parameter that reflects slight changes in the potential barrier shape or the effective electron mass. Especially in case of the low bias ohmic regime, J can be expressed approximately as

$$J \approx \frac{\sqrt{2m\Phi_B}\,e^2}{4\pi^2\hbar^2 d}\alpha V\exp\left(-\frac{2\sqrt{2m\Phi_B}}{\hbar}\alpha d\right) \qquad (2)$$

$$\beta_0 = \frac{2\sqrt{2m\Phi_B}}{\hbar}\alpha \qquad (3)$$

where β_0 is the decay coefficient, which reflects the exponential decrease of J versus molecule length (i.e. the width of the molecular tunnel barrier) in the low bias regime. However, note that these extracted fitting parameters, such as the decay coefficient or α from the Simmons model, do not imply certain exact quantitative meanings about the charge transport characterisics of the molecular junctions. Nonetheless, by analyzing the molecular transport junctions based on the model, we could gain a general idea of the charge transport characteristics of the junctions from a qualitative point of view.

To statistically investigate the charge characteristics of each working molecular junctions, we fitted (nonlinear least-squares fitting) the *J-V* characteristics of each working C8, C12 and C16 device in the Simmons tunneling model using equation (1) and obtained the transport parameters, including the Φ_B, α, and β_0 values. Here, each C8, C12 and C16 molecule has molecular lengths d of 13.3, 18.2 and 23.2 Å, respectively [21]. Based on the molecular lengths, we extracted the transport parameters, and figures 3(a) and (b) show the fitting results for the Φ_B and α values of all the individual working molecular devices. In addition, table 1 summarizes these parameters and J values at 1 V bias voltage that are averaged over all the working molecular devices. Note that the Φ_B and α values from the fitting results show relatively similar values despite the different molecular lengths. The α values were similar those from to previously reported studies, but the Φ_B values were not; instead, they showed higher values [10, 16]. Here, as mentioned previously, the α values do not possess an exact physical meaning, but they make the Simmons fitting on the molecular junctions possible by acting as an adjustable

parameter for the factors that one cannot take into account while modeling the tunneling junction as a rectangular barrier [20, 22, 23]. In addition, Φ_B reflects the relative energy alignment of the molecular frontier orbital with the electrode Fermi level, which depends on the nature of the contact properties at the molecule-electrode interface [24, 25]. Therefore, higher values of Φ_B may represent non-conformal contact properties of our molecular junction structure, which will result in an overall increase in the values [26, 27]. By applying these averaged parameters to equation (1), the estimated *J-V* characteristics for each molecular junction are presented as gray solid curves in figure 2(b), which show similar trajectories to the representative experimental data. In addition, the β_0 values extracted from all of the individual working devices using each Φ_B and α value are shown in figure 3(c). These values are found to be distributed in the range of 0.8–1.4 Å^{-1}, which are slightly larger values but mostly in agreement with previously reported β_0 values in pure (i.e. interlayer-less) M–M–M junction structures [10, 20–22]. It is noteworthy that the β_0 values from molecular junctions with interlayers, for example, the well-known conducting polymer PEDOT:PSS (poly(3,4-ethylenedioxythiophene) polystyrene sulfonate), show somewhat different values (0.5–0.6 Å^{-1}), which reflects the different natures of the contact properties (CH$_3$/Au versus CH$_3$/PEDOT:PSS) [8]. Using the representative *J-V* characteristics of the devices, one can determine the decay coefficient values from length-dependent analysis ($J \propto \exp(-\beta d)$) without modeling the molecular junction. Here, we used β (the value that was determined from the length dependent analysis) versus β_0 (the value that was determined from the Simmons tunneling model in the low bias regime, equations (2) and (3)) for comparison. For the length-dependent analysis, we plotted the J values of each molecular junction at bias voltages of 0.1 V to 1.0 V in 0.1 V increments versus the molecular length as shown in figure 3(d). Based on the fact that the J values show exponential dependence on the molecular length ($J \propto \exp(-\beta d)$), we could extract β values for each bias voltage from the magnitude of each linear fitting slope as shown in the inset in figure 3(d). From the analysis, we found that the averaged β value was approximately 1.1 Å^{-1}, which is in good agreement with previous studies on alkanethiolate molecular junctions [24]. Again, slightly larger values of β_0 from the Simmons fitting results may reflect the non-conformal contact properties of our molecular junction structure because of the strong dependence of the Simmons tunneling model on the $\alpha(\Phi_B)^{1/2}$ value (equation (3)) [24].

3.B. Length-dependent differences in the Gaussian deviations of the electrical characteristics

Based on the analysis of the representative charge transport characteristics of our molecular junctions, we investigated the length-dependent variation of electrical characteristics of the molecular junctions; specifically, the Gaussian standard deviation σ of the Gaussian fittings on the current density histogram as shown in figure 2(a). Here, the Gaussian fittings have been performed using a normal distribution function as
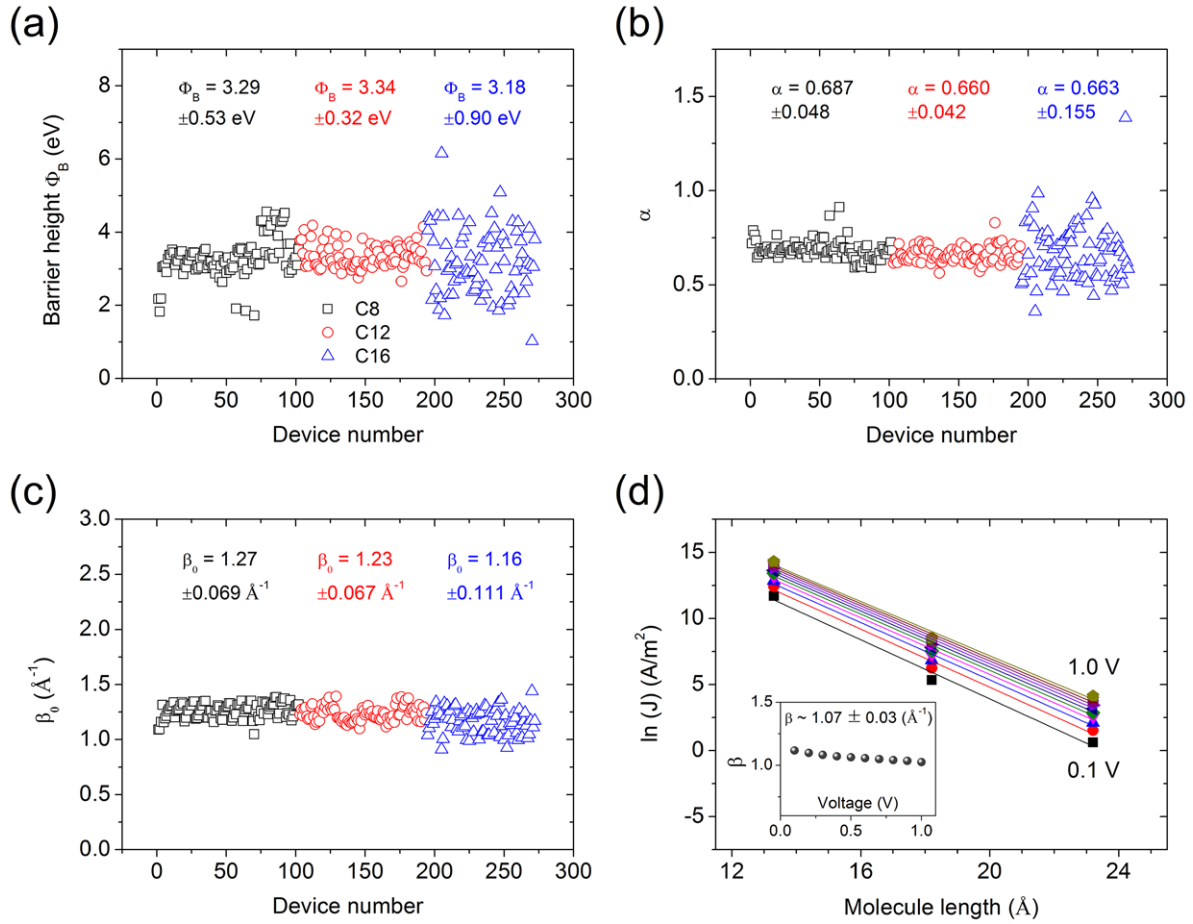
Figure 3. (a)–(c) Transport parameters derived from fitting the Simmons model for each individual working device. (a) Barrier height Φ_B, (b) adjusting parameter α, and (c) decay coefficient β_0. (d) Logarithmic current densities at bias voltages of 0.1 V to 1.0 V in 0.1 V increments versus the molecular length. Each solid linear line represents the exponential fitting results ($J \propto \exp(-\beta d)$). The inset depicts the deduced decay coefficient values (β) from the fitting results versus bias voltage.

Table 1. Summary of the statistically averaged transport parameters from all of the working molecular devices.

Molecules	J at 1 V (A m^{-2})	Φ_B (eV)	A	β_0 (Å^{-1})
C8	$\sim 1.62 \times 10^6$	3.29 ± 0.53	0.69 ± 0.05	1.27 ± 0.07
C12	$\sim 5.05 \times 10^3$	3.34 ± 0.32	0.66 ± 0.04	1.23 ± 0.07
C16	$\sim 6.22 \times 10^1$	3.18 ± 0.90	0.66 ± 0.15	1.16 ± 0.11

$$f(x) = \frac{1}{\sqrt{2\pi\sigma^2}} \exp\left\{-\frac{(x-\mu)^2}{2\sigma^2}\right\} \quad (4)$$

where μ is the Gaussian mean, and σ is its standard deviation. Then, as briefly mentioned above, the devices within a certain range of current density, depending on σ, can be considered working devices. Thus, the representative *J-V* characteristics could be derived in terms of statistically meaningful characteristics. Meanwhile, we also found that the degree of the distribution of the logarithmic *J* values of each molecular junction around the statistical mean value (i.e. the Gaussian mean μ) is dependent on the molecular length. Generally, this statistical distribution can be attributed to fluctuation factors causing such a distribution of tunneling current densities in molecular junctions. For example, these factors can be unexpected variations (i.e. fluctuations)

in the molecular configurations of the molecular layers in the junction, such as the tilting angle of the SAMs on the bottom electrode, surface roughness of the bottom electrode, existence of defects or contaminants, and contact properties at the metal-electrode interface [28–31]. Note that such variations may stem from parameters that are controllable during the junction fabrication process, such as variations in the junction area; however, this type of fluctuation could cancel out because all of the molecular junctions in this study are generated by single batch processes, i.e. all of the devices were made at the same time. Instead, variations in intrinsic parameters that are mostly uncontrollable in the molecular junction, for example, the tunneling pathway, are more likely to be the main reasons for the fluctuations in the statistical distribution [32]. A detailed discussion of this observation will be given in the following section.
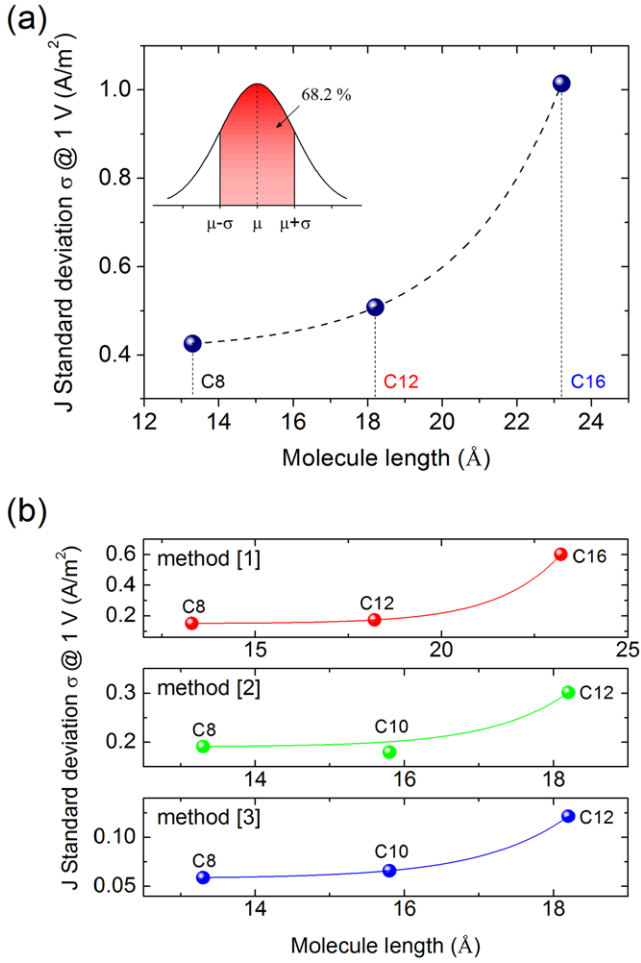
Figure 4. (a) A plot of the Gaussian standard deviation σ extracted from Gaussian fitting of the current density histograms versus the molecular length. Black dotted curve represents the exponential fitting results (see the main text). (b) Plots of the Gaussian standard deviation σ for different device fabrication methods [1–3]. The deduced parameter, detailed descriptions, and the information from [1–3] are presented in table 2.

Figure 4(a) shows the Gaussian standard deviation σ values of current density histograms at 1 V bias voltage for C8, C12 and C16 molecular junctions. As shown in the plot, the distribution of logarithmic J values depends on the molecular length, and the σ value increases as the molecular length increases. Here, to interpret the results quantitatively, we empirically assumed a simple exponentially dependent model of the σ value on molecular length as

$$\sigma = \sigma_0 + A \cdot \exp(\gamma d) \qquad (5)$$

where d is the molecular length, γ is a weighting factor, and σ_0 and A are adjusting factors. The idea of the model showing exponential dependence is based on the conformational degrees of freedom that are added to the alkyl chains with each methylene unit, which may accumulate to an exponential dependency of the overall structural configurations on the length. In statistical mechanics, the Boltzmann distribution describes the probability distribution of energy states as

$$f(E) = A \cdot \exp(-E/k_B T) \qquad (6)$$

where E is the energy of the state, k_B is the Boltzmann constant, and T is the temperature of the system. Then, if we consider the various conformational states (i.e. disordered configuration) of the individual molecules as specific energy states of the system, the total conformational degrees of freedom that are related to the number of accessible conformational states can be considered proportional to the maximum energy of the system. Meanwhile, the maximum energy of an individual molecule, for example, the alkanethiolates in this study, increases with the addition of each alkyl chain unit based on the repetitively connected spring model of a molecule in which the internal energy increases with the length d ($E \propto d^2$). Thus, the total conformational degrees of freedom of the molecule grow with the molecular length d due to the higher probability of various conformational states. Indeed, it is known from the theoretical studies that the conformational degree of freedom of an individual molecule increases with an increase in the number of bonding chains and, eventually, the molecular length in case of a repetitive structure [33]. Therefore, as a simple presumption, a specific charge transport parameter that is determined by the conformational degree of freedom can be modeled as a growth model with increasing molecular length. Note that we utilized SAMs instead of individual molecules; thus, the charge transport medium should have different dynamic characteristics due to intermolecular interactions [34]. Nevertheless, disorder in the SAMs due to the uncontrollable parameters that we mentioned above makes the SAMs imperfect, and this argument might be applicable to our molecular junction system. Focusing on this study, one of the most likely origins of the variations in the J-V characteristics through SAMs can be thought of as the variation in the width of the tunneling barrier based on the Simmons tunneling model. In this case, the molecule with longer lengths can produce larger variations in the thickness of the molecular layer than the shorter molecules due to intrinsic and extrinsic aspects, for example, more likely incorporation of defects and contaminants in the molecular layer or substantial molecular deformation due to the thicker cross-sectional area and higher structural degrees of freedom. Therefore, the thickness (i.e. the tunneling barrier width in terms of the Simmons tunneling model) of the molecular layer and, thus, the J-V characteristics that depend on the thickness might be proportional to the molecular length. Based on these observations, we empirically assumed that σ can be modeled as exponentially dependent on the molecular length d with a variable weighting factor γ. Though it is difficult to precisely define the physical implications of the γ value, this parameter reflects the relative strength of the dependence of the σ value on the molecular length. By applying this model to the σ values of C8, C12, and C16 devices, we plotted a fitting curve for C8, C12 and C16 as a black dotted curve in figure 4(b), which is in good agreement with the experimental data. However, we emphasize that there should be a rigorous quantitative explanation for the exponential dependence of the modeling based on molecular dynamics studies using the total interatomic potential of conformational energy [35, 36] or DFT calculations [37, 38].

Short chain molecule

Long chain molecule
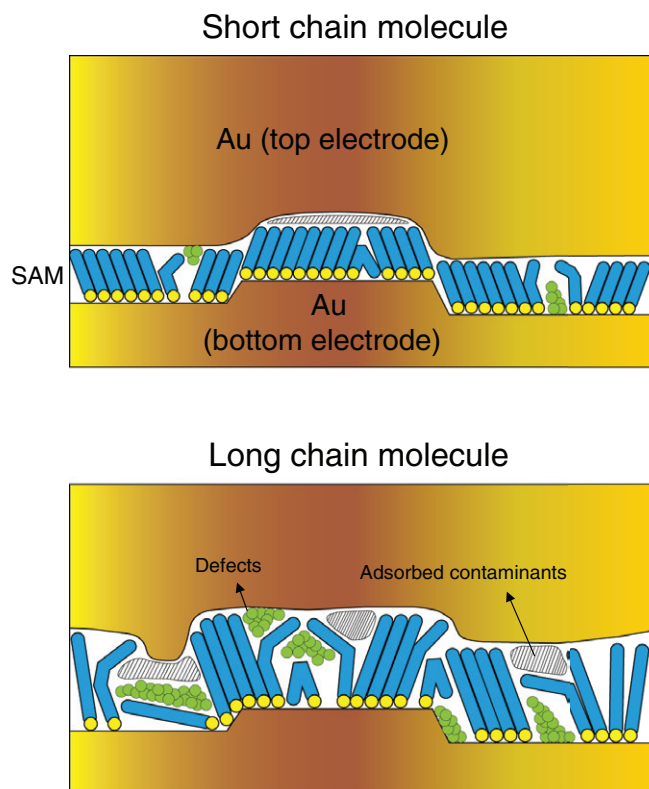
Figure 5. Schematic illustration of the molecular junction structures formed via the DMT method for both short and long chain molecules.

To visualize the above discussion, we suggested a schematic illustration of our fabricated junction for cases with short chain molecules and long chain molecules, including examples of defects and contaminants in the substrate, SAMs, and top electrode that can affect the molecular configuration, which is shown in figure 5. Usually, it is known that molecules with longer chains are incorporated via van der Waals attractions and form more ordered and dense molecular layers than short chain molecules [34]. However, because of the thicker cross-sectional areas of longer chain molecules, as we mentioned above, it is probable that SAMs formed with these molecules more frequently have artificial defects and contaminants. In addition, longer alkyl chains can induce more back-bending of the top end units of the molecules (that is, the top end units of the molecules fold back, pointing towards the bottom electrode) as schematically depicted in figure 5 [39]. Especially in our case, these kinds of defects can be more frequently incorporated due to the mechanical nature of our molecular device fabrication procedure resulting in disordering in the SAMs. For example, substrate-induced defects can be formed in the SAMs due to large grain boundaries from small grains on the surface of the bottom contact, and the top contact can also induce defects in the SAMs. Due to the mechanical processes used in the preparation of the top contact layer, the top contact surface might contain mechanical defects, such as metal particles. These kinds of defects result in poor contact with the SAMs, which cause variations in the electrical characteristics. Therefore, in spite of the possibility of better ordering of molecules with longer molecular chains, the effects of molecular

configuration disordering that result from artificial defects and contaminants may surpass the intermolecular interaction, which result in a larger variation in the electrical transport characteristics. Note that the different molecular conformations may also result from the intrinsic chemical properties of each molecule, such as the reactivity of the thiol groups or differences in orientation. Because each molecule has a different number of alkyl units, the reactivity of the thiol groups on the Au electrode surface varies due to the different thermodynamics. Specifically, there is a strong preference for the adsorption of the longer thiols than the shorter ones [40]. This property can also be observed from the results obtained by analytical chemistry [41, 42]. Therefore, in our case, there is a possibility that the C8 molecules form more imperfect SAMs than the longer molecules, which might result in a larger deviation in electrical characteristics. However, as we mentioned in the experimental section, we immersed the clean Au electrode into a dilute ethanolic solution of the alkanethiolate for enough time (24–48 h) to generate the full coverage structure of a densely packed monolayer of standing molecules for each molecular length [43]. Thus, the different reactivities of thiols with different molecular lengths may have only a slight effect on the deviation of the electrical characteristics; instead, other properties, for example, the incorporation of defects and disorder in the SAMs will have a dominant effect. Second, there is a chain-length dependent distinction of the structures and phases of the alkanethiolate SAMs [44]. However, slight differences in the overall structures and phases cannot change the electrical properties dramatically. The structural and morphological characterization results for the SAMs on the Au surface using scanning electron microscopy (SEM), atomic force microscopy (AFM) and x-ray diffraction (XRD) are shown in the supplementary data (stacks.iop.org/JPhysCM/28/094003/mmedia).

To identify this effect in other similar molecular junction structures, we compared the fitting results for the σ values in our previously reported studies using alkanethiolate molecules but different device fabrication methods. Figure 4(b) shows a plot of three different kinds of fitting results using equation (5) assembled using a similar device fabrication technique, i.e. vertical type microfabricated molecular junctions. As shown in the plot, each method shows good agreement with the fitting curves and different weighting factors, γ, below unity. Roughly speaking, it implies that the degree of molecular configuration disordering couldn't exceed the length of each molecule. The summary of the fitting results is presented in table 2. Note that there have been other studies in which the standard deviation (or full width at half maximum) of the Gaussian distribution of current density does not change monotonically with the molecular length and, therefore, disagree with our argument [8, 11, 45]. The reasons for the disagreement can be analyzed based on the following factors: (1) The distribution of the current density can be affected by not only the effects of molecular configuration disordering resulting from artificial defects and contaminants but other parameters, for example, the surface morphology of the bottom electrode, different SAM deposition times and environments, etc. Therefore, in other cases, these parameters

Table 2. Summary of the parameters deduced from the exponential fitting results of the σ values and detailed descriptions of the different fabrication methods.

Method #	Type of junction	Technique	γ	Ref.
[1]	Au-SAMs/Au	evaporated Au/ micropore	0.59	[46]
[2]	Au-SAMs/ polymer-Au	PEDOT:PSS/ micropore	0.98	[47]
[3]	Au-SAMs/ rGO-Au	solution-processed rGO	0.87	[13]
This work	Au-SAMs/Au	Direct metal transfer	0.36	

could be controllable factors for the deviation rather than uncontrollable factors. (2) Ultra clean junctions, i.e. defect-free molecular junctions, can be achieved using different molecular junction fabrication methods that are almost free from the degradation of electrical characteristics that result from artificial defects [45]. (3) The molecular devices for the comparison should be generated in a single batch; in other words, the devices with different molecular lengths should be formed at the same time so that all of the environmental parameters that are likely to change the quality of the molecular junctions are the same. Therefore, the solid-state molecular junctions fabricated using our molecular junction fabrication method and the other methods in figure 4(b) were synthesized in single batches. (4) The manner of colleting the *J-V* characteristics statistically can be different. In the case of our measurements, we obtained only one *J-V* trajectory per molecular junction, but in other cases, several trajectories were collected by repeating the *J-V* measurement on few molecular junctions, which can result in significantly different results depending on the junction selection [11].

4. Summary and conclusions

In summary, we have analyzed alkanethiolate molecular electronic junctions fabricated using our high yield molecular device fabrication method (DMT method) in terms of the electrical transport characteristics. In particular, we collected statistically significant transport parameters based on the Simmons tunneling model and determined representative current–voltage characteristics for the molecular junctions. The parameters mostly agreed well, but the barrier heights showed somewhat higher values, reflecting the non-conformal contact of the molecule-electrode interfaces in the molecular junctions. Additionally, we examined the statistical variations of the length-dependent electrical characteristics, especially the Gaussian standard deviation value σ. From the results, the σ values increase as the molecular length increases, and the relation might could be expressed using an exponential growth model based on empirical analysis. Finally, the probable origin of the length-dependent statistical variation could be related to artificial defects and contaminants in the molecular junctions. These observations may help pave the way for

the development of robust and stable molecular electronic junctions.

References

[1] Reed M A and Lee T 2003 *Molecular Nanoelectronics* (Stevenson Ranch: American Scientific)
[2] Chen J, Reed M A, Rawlett A M and Tour J M 1999 *Science* **286** 1550
[3] Collier C P, Wong E W, Belohradsky M, Raymo F M, Stoddart J F, Kuekes P J, Williams R S and Heath J R 1999 *Science* **285** 391
[4] Park J *et al* 2002 *Nature* **417** 722
[5] Nitzan A and Ratner M A 2003 *Science* **300** 1384
[6] Green J E *et al* 2007 *Nature* **445** 414
[7] Jiang J, Lu W and Luo Y 2004 *Chem. Phys. Lett.* **400** 336
[8] Akkerman H B, Blom P W M, de Leeuw D M and de Boer B 2006 *Nature* **441** 69
[9] Venkataraman L, Klare J E, Nuckolls C, Hybertsen M S and Steigerwald M L 2006 *Nature* **442** 904
[10] Kim T W, Wang G N, Lee H and Lee T 2007 *Nanotechnology* **18** 315204
[11] Reus W F, Nijhuis C A, Barber J R, Thuo M M, Tricard S and Whitesides G M 2012 *J. Phys. Chem.* C **116** 6714
[12] Wang G, Kim Y, Choe M, Kim T W and Lee T 2011 *Adv. Mater.* **23** 755
[13] Seo S, Min M, Lee J, Lee T, Choi S Y and Lee H 2012 *Angew. Chem. Int. Ed.* **51** 108
[14] Jeong H *et al* 2015 *Nanotechnology* **26** 025601
[15] Jeong H *et al* 2015 *Appl. Phys. Lett.* **106** 063110
[16] Wang W Y, Lee T and Reed M A 2003 *Phys. Rev.* B **68** 035416
[17] Zhitenev N B, Erbe A and Bao Z 2004 *Phys. Rev. Lett.* **92** 186805
[18] Simmons J G 1963 *J. Appl. Phys.* **34** 1793
[19] Wold D J and Frisbie C D 2001 *J. Am. Chem. Soc.* **123** 5549
[20] Cui X D, Zarate X, Tomfohr J, Sankey O F, Primak A, Moore A L, Moore T A, Gust D, Harris G and Lindsay S M 2002 *Nanotechnology* **13** 5
[21] Wold D J, Haag R, Rampi M A and Frisbie C D 2002 *J. Phys. Chem.* B **106** 2813
[22] Holmlin R E, Haag R, Chabinyc M L, Ismagilov R F, Cohen A E, Terfort A, Rampi M A and Whitesides G M 2001 *J. Am. Chem. Soc.* **123** 5075
[23] Rampi M A and Whitesides G M 2002 *Chem. Phys.* **281** 373
[24] Wang W Y, Lee T and Reed M A 2005 *Rep. Prog. Phys.* **68** 523
[25] Beebe J M, Kim B, Frisbie C D and Kushmerick J G 2008 *ACS Nano* **2** 827
[26] Majumdar N, Gergel N, Routenberg D, Bean J C, Harriott L R, Li B, Pu L, Yao Y and Tour J M 2005 *J. Vac. Sci. Technol.* B **23** 1417
[27] Wang G, Yoo H, Na S I, Kim T W, Cho B, Kim D Y and Lee T 2009 *Thin Solid Films* **518** 824
[28] Xu B Q and Tao N J J 2003 *Science* **301** 1221
[29] Engelkes V B, Beebe J M and Frisbie C D 2005 *J. Phys. Chem.* B **109** 16801

[30] Hu Y B, Zhu Y, Gao H J and Guo H 2005 *Phys. Rev. Lett.* **95** 156803

[31] Loertscher E, Weber H B and Riel H 2007 *Phys. Rev. Lett.* **98** 176807

[32] Song H, Lee T, Choi N-J and Lee H 2008 *J. Vac. Sci. Technol.* B **26** 904

[33] Rudnicki W R, Lesyng B and Harvey S C 1994 *Biopolymers* **34** 383

[34] Xiao X D, Hu J, Charych D H and Salmeron M 1996 *Langmuir* **12** 235

[35] Jimenez A, Sarsa A, Blazquez M and Pineda T 2010 *J. Phys. Chem.* C **114** 21309

[36] Chang W-Y, Fang T-H and Fang C -N 2009 *J. Phys. Chem.* B **113** 14994

[37] Torres E 2009 DFT study of alkanethiol self-assembled monolayers on Gold(1 1 1) surfaces *PhD Thesis* Graz University of Technology

[38] Alexiadis O, Harmandaris V A, Mavrantzas V G and Site L D 2007 *J. Phys. Chem.* C **111** 6380

[39] Nerngchamnong N, Yuan L, Qi D-C, Li J, Thompson D and Nijhuis C A 2013 *Nat. Nanotechtol.* **8** 113

[40] Bain C D and Whitesides G M 1989 *J. Am. Chem. Soc.* **111** 7164

[41] Finklea H O 1996 *Electroanalytical Chemistry* (New York: Marcel Dekker) vol 19, p 109

[42] Finklea H O 2000 *Encyclopedia of Analytical Chemistry: Applications, Theory and Instrumentation* (New York: Wiley)

[43] Love J C, Estroff L A, Kriebel J K, Nuzzo R G and Whitesides G M 2005 *Chem. Rev.* **105** 1103

[44] Fenter P, Eisenberger P and Liang K S 1993 *Phys. Rev. Lett.* **70** 2447

[45] Weiss E A, Chiechi R C, Kaufman G K, Kriebel J K, Li Z, Duati M, Rampi M A and Whitesides G M 2007 *J. Am. Chem. Soc.* **129** 4336

[46] Wang G, Kim T-W, Lee H and Lee T 2007 *Phys. Rev.* B **76** 205320

[47] Park S, Wang G, Cho B, Kim Y, Song S, Ji Y, Yoon M-H and Lee T 2012 *Nat. Nanotechnol.* **7** 438